Basic Analysis of an Air Breathing Electric Propulsion Concept

IEPC-2022-468

Presented at the 37th International Electric Propulsion Conference
Massachusetts Institute of Technology, Cambridge, MA, USA
June 19-23, 2022

Matthew S. Feldman[1] and Rostislav Spektor[2]
Viridian Space Corporation, El Segundo, CA, 90245, USA

Increased investment in observation and communication satellites is responsible for the resurgent interest in satellite air-breathing electric propulsion research, which refers to a concept where a scoop collects atmospheric gas at the front of the satellite and supplies it to a plasma thruster that produces sufficient thrust to overcome atmospheric drag. This paper discusses a methodology to analyze system and mission requirements for a satellite flying below 300 km, where an air-breathing propulsion system may become useful. As a case study we investigate adding an air-breathing propulsion system to a satellite of similar design to the ESA's Gravity Field and Steady-State Ocean Circulation Explorer (GOCE) that flew below 300 km. We find that scoop collection efficiency and compression ratio, thruster efficiency and specific impulse, and available orbit-averaged power are five key parameters influencing performance of the system. We also discuss concepts of operation of an air-breathing satellite in various orbits. Finally, we study basic system requirements for a refuelable space tug and show that a GOCE-like satellite could be refuelled for a round-trip mission from 300 km to 500 km in just under one year.

I. Nomenclature

$A_{sat,in}$	=	cross-sectional area of satellite or inlet
C_D	=	coefficient of drag
D	=	propellant collection divert ratio
F_D	=	drag force (on satellite)
g	=	gravitational constant of earth
h	=	altitude above Earth's surface
I_{sp}	=	specific impulse
m	=	particle mass
$\dot{m}_{in,c,T}$	=	mass flow (at inlet, collected, and to thruster)
$M_{E,p,sat}$	=	mass of Earth, propellant, satellite
n_{atm}	=	atmospheric density
P_T	=	power to thruster
Q	=	thruster duty cycle parameter
r_s	=	scoop compression ratio
R_E	=	radius of Earth
T	=	thrust
v_{orb}	=	orbital velocity
Δv	=	orbital maneuver delta-v
η	=	air-breathing electric propulsion mission efficiency metric
η_{sa}	=	efficiency of solar arrays

[1]Chief Technology Officer, matthew@viridianspace.com
[2]Chief Executive Officer, slava@viridianspace.com

η_s = scoop collection efficiency
η_t = thrust efficiency
τ_f = satellite fill-up time
ϕ = solar energy flux

II. Introduction

The availability of cheaper launch services at the beginning of the twenty first century marked rapid development of the space economy. Specifically, two types of services, satellite broadband communication and Earth Observation (EO), are receiving significant investments from both commercial and government sectors. While Geostationary Earth Orbit (GEO) and Medium Earth Orbit (MEO) were historically the first to be commercialized and widely used, Low Earth Orbit (LEO) is increasingly becoming a domain of commercial and military competition. Satellites flying closer to Earth have multiple economic and military advantages. They can provide higher resolution Earth Observation (EO) platforms for optical and electromagnetic surveillance, lower latency communication networks, and agile distributed assets for military purposes.

The emergence of the SpaceX StarLink, Amazon Kuiper, and OneWeb LEO broadband communication constellations highlights one particular business case for low flying satellites. In many areas of the world and even the US, satellite broadband is the only available type of communication service. Historically, communities living in these areas relied on broadband services supplied by GEO satellites. However, these satellites suffer from high latency (around 600 ms) due to the electromagnetic wave travel time to GEO, which eliminates real-time applications such as teleconferencing and gaming. As a result, the primary focus of these services was geared to one-way information flow, such as TV or radio broadcasting, where these established constellations generate up to $100B in annual revenue. The new LEO constellations aim to provide communication capabilities with latencies around 20-30 ms, similar to cable internet, enabling two-way live communication, gaming, and financial transactions through satellites. These constellations are being developed to orbit in multiple shells at altitudes between 1,200 km and 340 km. [1]

The last decade has also seen a rapid growth of low-flying satellites that provide Earth Observation (EO) services. Adoption of the CubeSat technology has helped to spark a revolution in EO services. Companies such as Planet, Spire, Iceye, and many others are able to launch their own constellations of small satellites and provide high resolution, high revisit rate EO services that up until now were the domain of government-sponsored and large corporation satellites. Typically, EO constellations orbit at around 500 km, which seems to provide the best balance between optical resolution and the rate of replenishing satellites due to the orbit decay induced by the atmospheric drag.

Significant improvements in EO and broadband communication can be achieved by lowering orbital altitudes to the 150–300 km range, which we will call Ultra-Low Earth Orbit (ULEO). For example, a factor of two optical resolution improvement can be achieved by lowering the altitude of an EO satellite from 500 km to 250 km. Similarly, a lower orbit can be beneficial for broadband communication satellites by reducing latency, increasing throughput, reducing antenna sizes, and decreasing power requirements. However, atmospheric drag becomes a significant challenge as the orbital altitude is decreased, requiring increased propulsion capabilities.

Yet, it is atmospheric drag that provides ULEO with an unique advantage. At this altitude Earth atmospheric drag is sufficiently strong to remove disabled satellites or debris within weeks, [2, 3] making this orbit self-cleaning. With increasing popularity of the proliferated LEO constellations, the idea of good orbital stewardship is becoming widely accepted by both government and commercial entities and may lead to a more restricted use of LEO orbits. Recent high-profile near misses between Starlink satellites [4, 5] and others [6] have highlighted fears that a collision cascade could permanently congest regions of LEO. On the other hand, ULEO constellations would be essentially immune to debris cascade concerns.

However, flying in ULEO below 300 km will require novel technologies that can enable satellites to overcome the increased aerodynamic drag while operating. This paper explores a propulsion system that is capable of indefinitely keeping a satellite at ULEO by utilizing Earth atmosphere as propellant. We also show that such a propulsion system can serve as an enabling technology for a refuelable space tug.

There are three key technical components that comprise the system: 1) A solar panel that provides electricity for an 2) Electric Propulsion (EP) device, which utilizes atmospheric gas that is fed to the thruster by 3) An efficient air scoop. Up until recently, technology was not sufficiently developed to allow creation of a viable air-breathing EP system. Each of the three components, however, has seen significant development in the last few decades to the point where air-breathing electric propulsion is close to becoming a reality.

There has been tremendous progress in the solar cell and solar panel technology. Solar cell efficiencies have improved from roughly 10% in 1970s to over 40% in 2000s. [7, 8] Thin and flexible substrate materials allow stowing larger solar arrays into the booster payload fairings. [9, 10] These improvements help support more powerful payloads and electric thruster capabilities.

Electric thrusters produce thrust by converting electric energy into kinetic energy in the propellant, and are capable of utilizing a variety of chemical elements and compounds. Most modern electric thrusters operate on xenon with efficiencies reaching 60%. [11, 12] Thrusters optimized for xenon have been operated with air at approximately 22% efficiency.[13] It is possible that further thruster design optimization for air may lead to higher operating efficiencies. However, the long-term effects of the oxygen environment on the thruster components have not yet been studied in detail. The electric thruster cathode may also require a redesign to operate on air as many currently used cathodes are prone to oxygen poisoning [11, 14, 15]. On the other hand, multiple contenders to overcome this challenge already exist, ranging from microwave and rf cathodes to electride cathodes [16–18].

The third key technological component is an air scoop. While very little attention was paid to this technology in the early days of air breathing EP development, recent experiments show some progress.[19] A few promising designs for the air-breathing EP scoops have been studied. One of the most notable studies has been performed by Barral *et al.*[20] and shows that a honeycomb scoop can reach compression ratio of around 300 at a collection efficiency of $\sim 30\%$.

In this paper, we develop key requirements for the holistic approach to the air breathing EP system design and explore the limits of current technology. The rest of the paper is organized as follows. Section III covers fundamental considerations and basic requirements for an air-breathing EP concept. Section IV discusses the requirements from the perspective of modern electric thruster technology. Section V reviews air-scoop requirements, and in Section VI we discuss a more advanced air-breathing EP system that enables space-tug missions.

III. Air Breathing Propulsion System Requirements

In this section we derive general propulsion performance requirements for a satellite that is using an air-breathing EP system to maintain orbit. For simplicity, we will assume that a satellite is flying in a purely circular orbit and that atmospheric conditions do not significantly vary throughout that orbit. Obviously, a more detailed study that does not rely on these assumptions will be needed for an actual mission design. We use the well-accepted NRLMSISE00 model (See Fig. 1) to describe the atmospheric gas conditions as a function of altitude.

A. Mathematical framework

The orbital velocity of a spacecraft circling Earth at an altitude h can be described as

$$v_{orb} = \sqrt{\frac{GM_E}{R_E + h}}, \tag{1}$$

where G is the gravitational constant and M_E and R_E are Earth mass and mean radius. At LEO, orbital velocity is around 7.8 km/s. The drag force acting on the satellite F_D is a function of the mean atmospheric density n_{atm} and atomic mass m, orbital velocity, drag coefficient C_D and the spacecraft cross-sectional area, A_{sat}:

$$F_D = \frac{1}{2} m n_{atm} v_{orb}^2 \left(C_{Dsat} A_{sat}\right), \tag{2}$$

where m and n_{atm} are altitude-dependent parameters.

The flow rate through the inlet m_{in} is proportional to the mean atomic mass, atmospheric density, orbital velocity, and the inlet area A_{in} according to the following relationship

$$\dot{m}_{in} = m n_{atm} v_{orb} A_{in}, \tag{3}$$

and the total collected propellant is dependent on the scoop efficiency, η_s, such that

$$\dot{m}_c = \eta_s \dot{m}_{in}. \tag{4}$$

These relationships allow us to rewrite the expression for the drag force in terms of the collected mass flow:

$$F_D = \frac{\dot{m}_c v_{orb}}{2\eta_s} C_D, \tag{5}$$

where for simplicity, we have adopted $C_D = C_{Dsat}(A_{sat}/A_{in})$.

To maintain orbit, the propulsion system must produce sufficient thrust to overcome the drag force expressed in Eq. (5). One way to do that is to produce thrust continuously throughout the orbit. In that case, the flow rate through the thruster may be as high as the collected flow rate $\dot{m}_c$. Alternatively, a satellite may collect gas throughout a portion of the orbital period in an onboard fuel tank and only thrust during a short portion of the orbit. We can define a duty cycle parameter, Q, to represent the ratio of thruster on-off times, such that $\dot{m}_T = Q\dot{m}_c$, where for a thruster firing continuously, $Q = 1$. And if a thruster is only fired for 10% of the orbit, $Q = 10$.

We can now define thrust necessary to overcome the drag force experienced during a single orbit as

$$T \geqslant \frac{1}{2} Q \dot{m}_{in} v_{orb} C_D. \tag{6}$$

Using $T = g\dot{m}_T I_{sp}$, we get:

$$g I_{sp} \geqslant \frac{v_{orb} C_D}{2\eta_s}, \tag{7}$$

where g is the Earth gravitational acceleration. Together, Eqs. (6) and (7) impose minimum performance requirements on a thruster. We note that this requirement is generic, and applicable to any air-breathing satellite system.

The power consumption of an electric propulsion device can be expressed in terms of thrust T, specific impulse I_{sp}, and thruster efficiency η_t, i.e.,

$$P_T = \frac{T g I_{sp}}{2\eta_t}. \tag{8}$$

Using Eqs. (6) and (7) we can derive the power requirement for an air-breathing EP satellite as

$$P_T \geqslant Q \frac{\dot{m}_{in} v_{orb}^2 C_D^2}{8\eta_t \eta_s}. \tag{9}$$

The orbit-averaged power requirement can then be written using equations above:

$$\langle P_T \rangle \geqslant \frac{\dot{m}_{in} v_{orb}^2 C_D^2}{8\eta_t \eta_s} = \frac{m n_{atm} v_{orb}^3}{8\eta_s \eta_t} C_D^2 A_{in}. \tag{10}$$

The power produced by a spacecraft solar array can be computed as a product of the solar energy flux ϕ, solar array area A_{sa} and solar array efficiency η_{sa} as

$$P_{sa} = \eta_{sa} \phi A_{sa} = \phi_{sa} A_{sa}, \tag{11}$$

where A_{sa} could be larger than the front-projected satellite cross-sectional area, A_{sat}, and ϕ_{sa} is the maximum power produced by the solar arrays per unit area. The orbit-averaged available power is then:

$$\langle P \rangle = \eta_p \phi_{sa} A_{sa}, \tag{12}$$

where η_p is a geometric efficiency factor that takes into account eclipses and non-optimum pointing of the solar arrays. In a perfectly sun-synchronous dusk-dawn orbit $\eta_p = 1$, and in the worst case eclipses and orientations, $\eta_p = 1/\pi$.

Combining Eqs. (10) and (12) we get

$$\eta = \eta_s \eta_t \geqslant \frac{m n_{atm} v_{orb}^3}{8\eta_p \phi_{sa}} C_D^2 \frac{A_{in}}{A_{sa}} = \frac{\dot{m}_{in} v_{orb}^2 C_D^2}{8\langle P \rangle}. \tag{13}$$

It is important to outline the following features of the equation above. First, $C_D^2(A_{in}/A_{sa})$ is constant for a given satellite geometry and orientation, since it only involves areas and the drag coefficient. Second, for fixed altitude (and for a given satellite design) the required thruster efficiency scales inversely with the scoop efficiency, as shown in Fig. 2. A less efficient thruster requires a more efficient scoop. We also note that orbital velocity is only a weak function of the orbital altitude h, since for LEO orbits $R_E \gg h$. On the other hand, atmospheric density n_{atm} is a strong function of altitude, as is the total collected propellant flow rate, $\dot{m}_c$.

Equation (13) is useful for selecting appropriate thruster and scoop performance for a given mission. The left hand side can be interpreted as the overall system efficiency, $\eta = \eta_s \eta_t$. And the right hand side has the useful property of being constant for a fixed satellite geometry and mission orbit.

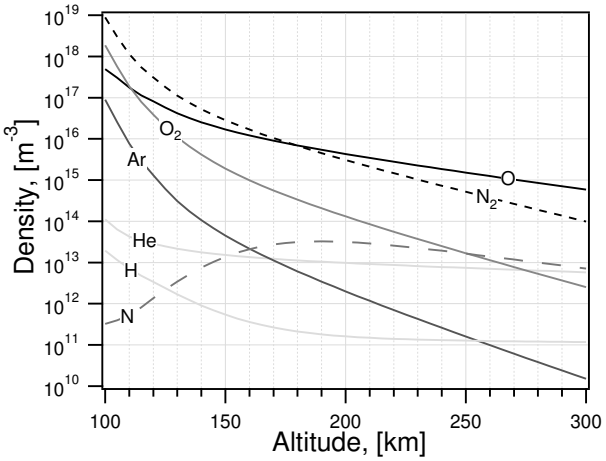

Fig. 1 NRL MSISE00 model results taken at zero latitude (equator) and zero longitude (prime meridian) at 8:03:20 on July 21st, 2009.

B. Atmospheric properties

Before proceeding further with analysing the system, we briefly describe the atmospheric model used in this study. Earth's atmosphere consists of various gas molecules whose concentration changes as a function of altitude, longitude and latitude, solar weather, and other factors. While there are many atmospheric models that predict species concentration, in this paper we use the NRL MSISE00 model, which relies on the ISO 14222 standard. Density distribution as a function of altitude for typical conditions is plotted in Fig. 1. The figure shows model results taken at zero latitude (equator) and zero longitude (prime meridian) at 8:03:20 on July 21st, 2009. We can see that above 180 km atomic oxygen dominates other atmospheric constituents. Nitrogen is the second dominant species, and below 180 km it dominates atomic oxygen. For the following analysis we use the total density n_{atm} and the mean atomic mass m at a given altitude to calculate mass flow rate, where the mean atomic mass is computed as

$$m = \frac{\sum_s m_s n_s}{n_{atm}}, \tag{14}$$

where the summation is performed over all species shown in Fig. 1. We should note that atomic oxygen may degrade satellite components. Japanese SLATS satellite, flown at ULEO, investigated the effects of atomic oxygen, but didn't find any significant materials degradation. [21, 22] Further studies are required to qualify needed materials for future satellites that will spend significant time at ULEO.

C. Trends in requirements

Recall that for a given spacecraft geometry, all of the salient propulsion requirements are determined by the mission altitude, and since the orbital velocity is only a weak function of altitude at LEO, these requirements are all primarily dependent on the density of the atmospheric gas.

One requirement that we have not yet mentioned, but that is critically important for efficient electric propulsion system performance, is the scoop compression ratio r_s. Electric propulsion devices need sufficient gas density n_{ig} to efficiency ignite and sustain a plasma discharge. This density is typically around $3 \cdot 10^{19}$ m^{-3}. Therefore, we place a compression ratio requirement on the air scoop that is determined by the fraction of n_{ig} and the incoming atmospheric gas density, such that

$$r_s \geqslant \frac{n_{ig}}{n_{atm}(h)}. \tag{15}$$

We now can point to four main parameters that together determine an air-breathing electric propulsion system performance for a given satellite geometry: scoop efficiency η_s, scoop compression ratio r_s, thruster efficiency η_t, and average available power $\langle P \rangle$. The first two parameters depend on the orbital altitude, h, but we can also express them

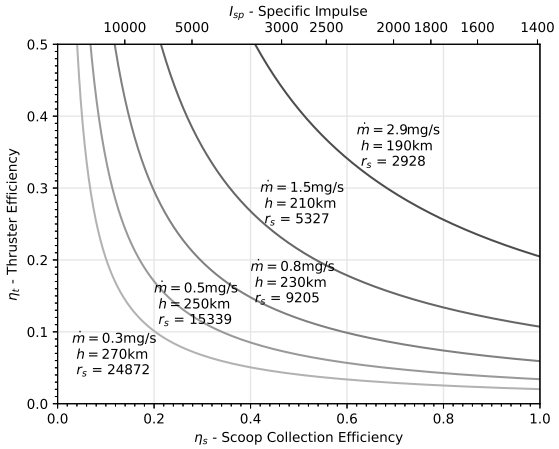

Fig. 2 Performance curves of required thruster efficiency as a function of scoop efficiency for varying altitudes assuming $\langle P \rangle$ = 1.3 kW, C_D = 3.5, and A_{in} = 1 m^2. The r_s for each line of constant altitude is shown.

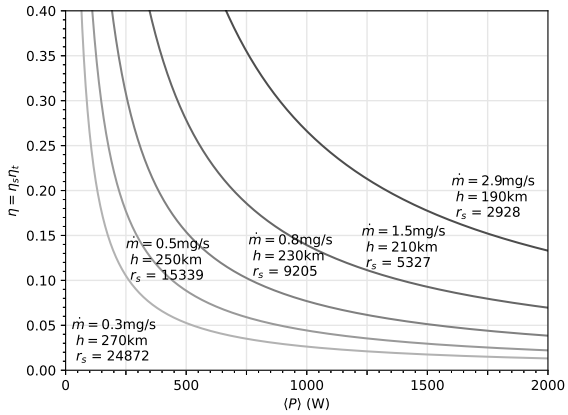

Fig. 3 Performance curves of required η as a function of $\langle P \rangle$ for varying altitudes assuming, C_D = 3.5, and A_{in} = 1 m^2. The r_s and $\dot{m}_{in}$ for each line of constant altitude is shown.

through the total mass flow incident on the inlet $\dot{m}_{in}$, which eliminates the need to explicitly define satellite geometric areas.

Before plotting some characteristic curves, let us point out two key features of satellite performance as a function of altitude. At low altitudes the atmospheric density eventually increases sufficiently that the right hand side of Eq. (13) exceeds 1, at which point even a perfectly efficient scoop and thruster could not maintain orbit with fixed power. At the other extreme, at higher altitudes, the atmospheric density becomes more rarified, requiring increased compression ratio in order to ignite the thruster. At some point that compression ratio exceeds the capability of the scoop performance. These two factors define an operational altitude envelope for air-breathing electric propulsion.

For the rest of this paper, we will base many example results around data and parameters from the GOCE mission, an ESA satellite that actually flew at ULEO altitudes [23, 24]. This satellite geometry was optimized to minimize drag and was propelled by a xenon-fueled ion thruster to offset drag. A few key parameters of interest from the GOCE mission are a drag coefficient, C_D = 3.5, an inlet area, A_{in} = 1 m^2, and end-of-life maximum available power of 1.3 kW. Using these parameters, and assuming a GOCE-like satellite configuration, the minimum altitude an air-breathing electric propulsion powered satellite could sustain would theoretically be around 150 km. However, this calculation assumes perfect thruster and scoop collection efficiency.

Figure 2 shows the required scoop efficiency, η_s, as a function of thruster efficiency η_t for varying lines of constant

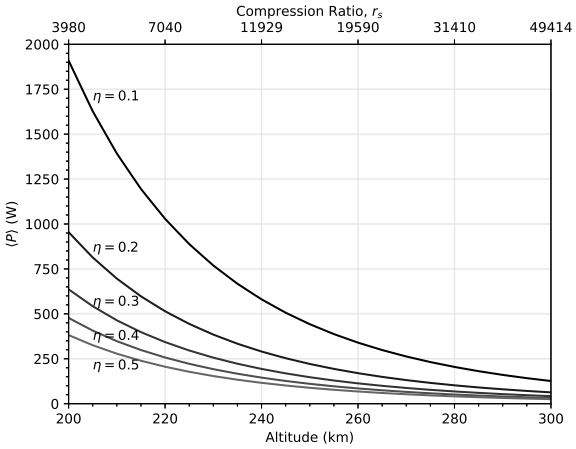

Fig. 4 Performance curves of required $\langle P \rangle$ as a function of altitude (and required r_s) for varying η assuming C_D = 3.5, and A_{in} = 1 m^2.

altitude at fixed power, as expressed by Eq. (13). In this plot, we assume that the available orbit-averaged power is 1.3 kW, the inlet area is 1 square meter, and C_D = 3.5. Like in above calculations, these values approximate the actual parameters taken from the GOCE mission [23, 24]. The altitude dependent data is taken from Fig. 1, and the associated compression ratios required to reach efficient ionization are listed next to each curve, together with the associated altitude and mass flow rate. At the top axis, the requirement on thruster specific impulse is related to scoop efficiency through Eq. (7).

This same data is replotted in Fig. 3 to show the mission efficiency metric, η, as a function of orbit averaged power for different inlet mass flow rates. In Fig. 4 we replot the same data one more time to show the orbit-averaged power requirement as a function of altitude and mission efficiency, η.

In order to contextualize these plots, the performance of the scoop and the electric thruster must each be understood. For example, typical scoops that have been proposed and tested consist of elongated honeycomb shapes and have demonstrated compression ratios up to 300 and collection efficiencies around 30 percent, with higher efficiency corresponding to lower compression ratio.

While electric thrusters are typically optimized to operate with xenon, these systems have been tested with a variety of gases, including oxygen and nitrogen. While operating with these air constituents, thruster efficiency has often been reduced by half or more, resulting in $\eta_t \sim 20 - 25\%$. [13, 25, 26]

IV. Electric Propulsion Requirement

There are three key thruster performance parameters that influence technology selection for the air breathing EP application: thrust, specific impulse, and efficiency. Thrust presents the most obvious requirement – the thruster must produce sufficient force to overcome drag. The specific impulse requirement, takes a bit more explanation. It is obvious that a thruster must produce specific impulse that is at least 780 s (v_{orb}/g). This statement simply states that on average particles must leave faster than they enter the system. However, in practice, specific impulse must be significantly higher than that. Equation (7) states that a system must produce specific impulse high enough to offset the momentum loss due to all the incoming particles striking the satellite, i.e. the drag. Thus, in reality exhaust velocity on the order of twice the orbital velocity or even more must be achieved by the thruster. For example, assuming C_D = 3.5 and scoop efficiency η_s = 0.3, Eq. (7) places the minimum specific impulse reqirement at 4,643 s. Such high specific impulse falls within the domain of electric propulsion. In particular, electrostatic and electromagnetic thrusters are capable of producing specific impulse in that range. Available literature indicates that electrothermal thrusters, such as arcjets, resistojets, and RF thrusters currently cannot achieve sufficient exhaust velocity to make a viable air-breathing EP system.

The typical workhorse thruster designs such as Hall Effect Thrusters (HETs) and Gridded Ion Thrusters (GIT) are capable of producing specific impulses around 2,000 s when operated with xenon. Recent literature [13] indicates that when operated with oxygen standard HETs, such as the SPT-100, can produce an I_{sp} within 5% of the I_{sp} produced with xenon at voltages between 300 V and 400 V, however that performance significantly degrades at lower voltages and

drops to only about 40% of that with xenon at 200 V.

The thruster efficiency requirement is closely related to scoop efficiency – a more efficient thruster allows a less efficient scoop, according to Eq. (13). Typical modern HET efficiency is around 50% when operated with xenon. That number applies for thrusters in the 1 – 4 kW range and drops to around 30% below roughly 500 W. This places a practical limitation on the size of the air-breathing system. A small system will be less efficient and may not even be feasible below a certain thruster power level. On the other hand, HETs operated at higher power with high operating voltage (400+ V) may be well suited for the air-breathing application. GITs may also provide sufficient performance for an air-breathing system, and typically achieve higher I_{sp} than HETs. They may also maintain some performance advantages at slightly lower powers. However, it is not clear if grid erosion will be a limiting factor for adopting these types of thrusters operating on oxygen. HETs share a similar oxygen-material compatibility concern. While the ceramic wall components may not be susceptible to oxidation, the anode material will need to be selected appropriately, and further engineering work may be required to improve overall lifetimes.

Furthermore, both HETs and GITs require cathodes. The current state-of-the-art cathode technology, hollow BaO or LaB6 cathodes are prone to oxygen poisoning and will not work with an air-breathing thruster. An oxygen-compatible cathode needs to be developed. Most obvious options are rf and microwave cathodes. However, these cathodes require input power and reduce the overall thruster efficiency even further.

V. Air Scoop Requirements

Multiple groups throughout the world are researching air-breathing EP technology. While many focus on developing a thruster capable of operating on low density oxygen, some groups have investigated scoop technology [19, 20, 27]. The performance of a scoop is controlled by three characteristic velocities and a variety of geometric factors. The velocities of interest are the spacecraft orbital velocity, which is the velocity at which atmospheric gas enters the scoop, v_o, the atmospheric gas thermal velocity v_{to}, and the velocity of particles that are thermalized by the impact with the scoop, v_t. Specifically, one may show [20] that compression ratio is proportional to the ratio of the orbital and thermal velocities, $r_s \sim v_o/v_t$, indicating that a higher compression ratio is achieved with cooler scoop temperature. This indicates that active scoop cooling may be an interesting area of research to improve the overall system.

The other velocity ratio, $S = v_o/v_{to}$ controls the incidence angle of the average orbital particle. For large S, particles enter the scoop fully aligned, but as S decreases, the incoming fast particles are more likely to hit the walls of the scoop. A typical scoop contains a honeycomb structure at the inlet with a large thermalizing chamber behind it. The idea behind the honeycomb structure is to increase the probability of transmitting the fast incoming particles to the back of the scoop and to reduce the probability of thermal particles backstreaming through collisions with the walls of the honeycomb. The optimization of a scoop then boils down to selecting the optimum honeycomb aspect ratio.

Another important parameter for a scoop operation is the outlet to inlet area fraction. [20] Decreasing the outlet area increases compression r_s but decreases the collection efficiency η_s. Barral *et al.* [20] showed that scoops reach compression ratios around 250 with oxygen and 350 with nitrogen. A scoop based on the design optimization by Barral *et al.* was constructed and tested by Sitael [19] and reported collection efficiency of 30%. No scoop compression ratio was reported, however the thruster was ignited and operated successfully during that experiment.

One intrinsic assumption made for the scoop analysis above was a perfect accommodation coefficient. This implies that all particles that strike a surface thermalize to that surface temperature. In practice, this assumption may not be strictly true, resulting in less efficient scoop performance. On the other hand, one study [28] aims to take advantage of incomplete accommodation through an elliptic wall geometry. This design tries to redirect fast particles directly to a narrow outlet area, thereby obtaining improved collection efficiency. Such a concept shows theoretical promise when only specular reflection is considered, but ignores many practical and fundamental considerations that may invalidate the conclusions. These ignored considerations include a thermal velocity spread of the incoming particles, imperfect accommodation, and other collisional processes that become important as compression is increased.

VI. Space Tug Mission Analysis

An advanced version of an air-breathing electric propulsion system may be able to siphon off excess propellant into a fuel tank for later use. For example, the excess propellant could be used to perform orbital inclination changes or excursions to higher altitudes (and back). With these capabilities, an air-breathing satellite can be designed as a reusable space tug or satellite servicing platform.

To function in such a capacity, an air breathing electric propulsion system must simultaneously use some of the

collected mass flow to maintain orbit while preserving the rest for later maneuvers. The exact dynamics of these maneuvers may become quite complicated. However, it is helpful to benchmark what might be achievable using our basic requirements model from Section III.

A. Maintaining Orbit while Diverting Propellant

In order to incorporate space-tugging capabilities in our propulsion system analysis we need to modify the equations in Section III to include two additional terms. The first term is a propellant divert ratio, D, that is the fraction of the collected mass diverted to the fuel tank for later use. The second term is the total satellite system dry mass, M_{sat}, which does not affect the basic requirements, but does affect how much Δv can be achieved for given propellant mass.

Note that M_{sat} actually includes the mass of the object to be maneuvered (such as a customer satellite) and the dry mass of the space tug itself. However, in some situations this mass may change throughout the mission. For example, when maneuvering to collect a piece of debris to de-orbit, the space tug would first only need adjust its own orbit to match the target, but after collecting the target, the mass considered would include for both the system and target combined. We ignore this distinction for the moment and use M_{sat} generically to understand the dynamics of the analysis.

The drag equation, Eq. (5), remains unchanged. However, the total propellant available for the thruster is now reduced:

$$\dot{m}_T = (1 - D)\dot{m}_c \tag{16}$$

where we have ignored the thruster operational duty cycle, Q, since it cancels out later in the calculations. The thrust requirement to maintain orbit, Eq. (6), remains unchanged. However, because the mass flow to the thruster has decreased, the I_{sp} requirement becomes:

$$gI_{sp} \geqslant \frac{v_{orb} C_D}{2(1 - D)\eta_s}. \tag{17}$$

Propagating this divert ratio through the previous analysis, we find that the new mission metric becomes:

$$\langle P \rangle \eta_t \eta_s \geqslant \frac{\dot{m}_{in} v_{orb}^2 C_D^2}{8(1 - D)}. \tag{18}$$

That is, if we wish to divert some fraction of the collected propellant into a fuel tank, we must increase the thruster I_{sp} accordingly.

Before proceeding, we can note that an optimum divert ratio, D, can be derived quite simply. First, note that the rate at which mass is stored in the propellant tank is,

$$\dot{m}_f = \dot{m}_c - \dot{m}_T = D\dot{m}_c. \tag{19}$$

Combining with Equations 4 and 18, we find that

$$\dot{m}_f < \frac{8\langle P \rangle \eta_t \eta_s^2}{v_{orb}^2 C_D^2} D(1 - D). \tag{20}$$

For a fixed available power and air-breathing electric propulsion system performance metrics, this fill-up rate is maximized by optimizing the $D(1 - D)$ term, which occurs when $D = 0.5$.

B. Non-Orbit Keeping Maneuvers

An orbital maneuver can be characterized by the change in spacecraft velocity required to accomplish that maneuver. That change in velocity is called Δv. We calculate the achievable Δv for an air-breathing system as a function of the system performance and divert ratio.

Recall the rocket equation that calculates Δv in terms of the total satellite and propellant masses:

$$\frac{M_p}{M_{sat}} = \exp^{\Delta v / g I_{sp}} - 1, \tag{21}$$

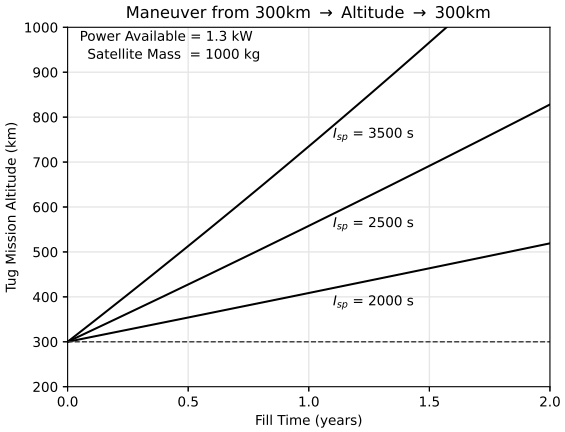

Fig. 5 Refuelable space tug round trip altitude capability versus the fill up time at 300 km. Calculation assumes a GOCE-like satellite body.

where M_p is the total propellant mass required for a maneuver and M_{sat} is the satellite dry mass that excludes M_p. Solving for Δv, we get:

$$\Delta v = g I_{sp} \ln(\frac{M_p}{M_{sat}} + 1) \tag{22}$$

Rewriting M_p in terms of the fill rate and fill time τ_f.

$$M_p = \dot{m}_f \tau_f \tag{23}$$

and using Eq. (17), we get that

$$\Delta v = \frac{1}{1-D} \frac{v_{orb} C_D}{2\eta_s} \ln(\tau_f \dot{m}_{in} \eta_s D / M_{sat} + 1). \tag{24}$$

In the above equation, we have assumed gI_{sp} is identical to the I_{sp} used during the re-fueling portion of the mission described above in Eq. (17). In practice, this assumption may not be accurate. During a maneuver, extra thrust is required beyond that which negates drag. If we have a fixed power $\langle P \rangle$, and use more mass flow in the same thruster, I_{sp} will decrease if η_t remains constant. Alternatively, in order to keep a fixed I_{sp} with higher mass flow rate, more power may be required.

Equation (24) is a complicated function that describes the size of a maneuver Δv that can be performed as a function of fill up time, τ_f. It can alternatively be solved for τ_f, such that

$$\tau_f = \frac{M_{sat}}{\dot{m}_{in} \eta_s D} \left(e^{(1-D)\frac{2\eta_s}{C_D}\frac{\Delta v}{v_{orb}}} - 1 \right) \tag{25}$$

In Eq. (25), we note that as long as $\Delta v \ll v_{orb}$, the exponential can be Taylor expanded using $e^x \approx 1 + x$. The approximation is reasonable for some low Δv maneuvers, but may not be for extreme LEO to GEO maneuvers. Note that this requirement is identical to saying that $\Delta v \ll gI_{sp}$ since I_{sp} in our derivation is proportional and indeed greater than v_{orb}.

Armed with this assumption, we can now derive an optimistic performance relationship between τ_f and Δv.

$$\Delta v \approx \frac{D}{1-D} \frac{C_D}{2} v_{orb} \frac{\dot{m}_{in}}{M_{sat}} \tau_f. \tag{26}$$

The above equation tells us the maximum Δv achievable in a given fill up time τ_f as a function of the mass flow into the system, the divert ratio, and the total satellite mass.

Note that the divert ratio, D, is not arbitrarily controllable. Because the thruster must produce sufficient I_{sp} to overcome the drag force, in practice this ratio is defined by the achievable I_{sp} of the thruster. If we use Eq. (7) to define the minimum $I_{sp_{min}}$ necessary to maintain orbit with $D = 0$, we can calculate the fill up time as

$$\Delta v \approx (I_{sp}/I_{sp_{min}} - 1)\frac{C_D}{2} v_{orb} \frac{\dot{m}_{in}}{M_{sat}} \tau_f. \tag{27}$$

Using Eq. (18), we can re-write the performance requirement as

$$\dot{\Delta v} = \frac{\Delta v}{\tau_f} \approx \frac{4D}{v_{orb} C_D M_{sat}} \langle P \rangle \eta_t \eta_s. \tag{28}$$

Alternatively,

$$\dot{\Delta v} \approx \frac{2\langle P \rangle \eta_t}{M_{sat}} \left(\frac{1}{I_{sp_{min}}} - \frac{1}{I_{sp}} \right), \tag{29}$$

where $\dot{\Delta v}$ is the maximum possible rate at which a tank could be filled in terms of mission Δv requirements.

Consider a satellite similar to GOCE, that has a mass M_{sat} = 1,000 kg, an end of life orbit-averaged power (accounting for eclipse) of $\langle P \rangle$ = 1.3 kW, and a drag coefficient C_D = 3.5. If we assume that a mission metric of $\eta = \eta_t \eta_s = 0.2$ and $D = .5$ are possible, we find the maximum $\dot{\Delta v}$ achievable is 600 m/s/year. For reference, this is more than twice the Δv required for a round trip from 300 km to 500 km. That is, a GOCE like satellite could fully refuel for a mission from ULEO to LEO and back with just under half a year of atmospheric refueling. In Figure 5, we relate τ_f to Δv and the equivalent mission profiles for various thruster specific impulses.

VII. Conclusions

This paper discusses air-breathing electric propulsion as an enabling technology to allow satellites to fly at altitudes below 300 km, which we call Ultra Low Earth orbit (ULEO). Such technology is necessary to overcome the atmospheric drag forces associated with these low orbits without running out of propellant. We began by analyzing the basic system and mission requirements for a satellite powered with air-breathing electric propulsion and showed that system viability is primarily dependent on five key performance parameters.

- Scoop Efficiency, η_s - the fraction of incident mass flow collected by the scoop to be fed to the thruster.
- Scoop Compression Ratio, r_s - the ratio of the incoming atmospheric density and the gas density fed to the thruster.
- Thruster Efficiency, η_t - the fraction of power converted to kinetic energy in the thruster.
- Thruster Specific Impulse, I_{sp} - the average exhaust speed of the thruster which must be greater than the incoming atmospheric orbital flux speed.
- Orbit Average Power, $\langle P \rangle$ - the power available for oribt keeping, not reserved for mission payload.

From these performance parameters, we derived the system requirements necessary to reach “break-even", where net thrust is greater than net drag.

Next, we reviewed the available literature on performance of modern electric thrusters on oxygen and nitrogen, which revealed that thruster efficiencies around 20% is likely achievable at moderate power requirements of 1 – 2 kW. More efficiency may be obtainable for thrusters specifically designed for operation on air. We also reviewed the performance for scoops that have been investigated by numerous authors.

In our final section, we described a refuelable space-tug enabled by the air-breathing electric propulsion – where extra propellant collected from atmosphere can be stored for later use. Such a satellite would be able to perform a mission, then descend back to ULEO to refuel. To do this, we described the modifications necessary to the basic system requirements in order to divert some incoming mass flow to a fuel storage tank (rather than directly to the thruster). This analysis showed that refueling times for missions from ULEO to LEO and back would be on the order of a half a year, allowing a single vehicle to perform many such missions over the course of its life.

References

[1] McDowell, J. C., “The Low Earth Orbit Satellite Population and Impacts of the SpaceX Starlink Constellation,” *The Astrophysical Journal*, Vol. 892, No. 2, 2020, p. L36. https://doi.org/10.3847/2041-8213/ab8016, URL https://doi.org/10.3847/2041-8213/ab8016.

[2] Strizzi, J. D., "AN IMPROVED ALGORITHM FOR SATELLITE ORBIT DECAY AND RE-ENTRY PREDICTION," Aeronautics and astronautics, Massachusetts Institute of Technology, 1993.

[3] Goldman, D., "Mitigation of Orbital Debris in the New Space Age," Presentation IB Docket No. 18-313, SpaceX, August 2021.

[4] Retrieved 2021. Https://www.msn.com/en-gb/news/world/spacex-e2-80-99s-starlink-satellites-near-misses-with-other-spacecraft-are-getting-e2-80-98out-of-control-e2-80-99-experts-say/ar-AANybG4.

[5] Retrieved 2021. Https://www.businessinsider.com/starlink-will-ultimately-account-for-90-of-orbital-near-misses-2021-8.

[6] Retrieved 2021. Https://metro.co.uk/2019/09/02/elon-musks-spacex-starlink-satellites-almost-hit-esa-spacecraft-10672608/.

[7] NREL, "Best Research-Cell Efficiencies," , Retrieved 2021. Https://www.nrel.gov/pv/cell-efficiency.html.

[8] Surampudi, R., Blosiu, J., Stella, P., Elliott, J., Castillo, J., Yi, T., Lyons, J., Piszczor, M., McNatt, J., Taylor, C., Gaddy, E., Liu, S., Plichta, E., Iannello, C., Beauchamp, P., and Cutts, J., "Solar Power Technologies for Future Planetary Science Missions," report JPL D-101316, JPL, December 2017.

[9] Banik, J., and Hausgen, P., "Next Generation Flexible Solar Array Technology for DOD Spacecraft," 2017. https://doi.org/10.2514/6.2017-5307, presented at 107 AIAA SPACE Forum, 12–14 September, 2017, Orlando, Florida, AIAA-2017-5307.

[10] Chamberlain, M. K., Kiefer, S. H., and Banik, J., "On-orbit Structural Dynamics Performance of the Roll-Out Solar Array," 2018. https://doi.org/10.2514/6.2018-1942, presented at 2018 AIAA Spacecraft Structures Conference, 8–12 January, 2018, Kissimmee, Florida, AIAA-2018-1942.

[11] Goebel, D. M., and Katz, I., *Fundamentals Of Electric Propulsion: Ion And Hall Thrusters*, John Wiley & Sons Inc, Hoboken, NJ, USA, 2008.

[12] Jackson, J., Miller, S., Cassady, J., Soendker, E., Welander, B., Barber, M., and Peterson, P., "13kW Advanced Electric Propulsion Flight System Development and Qualification," . Presented at the 36^{th} International Electric Propulsion Conference, Vienna, Austria, 15-20 September 2019, IEPC-2019-692.

[13] Khartov, S., Napolov, D., Perfiliev, A., and Zikeeva, J., "Experimental investigation of the alternative propellants for stationary plasma thruster," 2000. Proc. of the 3rd International Conference on Spacecraft Propulsion.

[14] Springer, R. W., and Haas, T. W., "Auger electron spectroscopy study of cathode surfaces during activation and poisoning. I. The barium-on-oxygen-on-tungsten dispenser cathode," *J. Applied Phys.*, Vol. 45, No. 12, 1974, pp. 5260–5263. https://doi.org/10.1063/1.1663226.

[15] Marrian, C., and Shih, A., "The operation of coated tungsten-based dispenser cathodes in nonideal vacuum," *IEEE Transactions on Electron Devices*, Vol. 36, No. 1, 1989, pp. 173–179. https://doi.org/10.1109/16.21202.

[16] Weatherford, B. R., and Foster, J. E., "Initial Performance of a ECR Waveguide Plasma Cathode with Permanent Magnets," . Presented at the 31^{st} International Electric Propulsion Conference (IEPC), Ann Arbor, MI, USA Sep. 20–24, 2009. IEPC-2009-211.

[17] Rand, L. P., "A CALCIUM ALUMINATE ELECTRIDE HOLLOW CATHODE," Ph.d, Colorado State University, 2014.

[18] Tsay, M., Model, J., Barcroft, C., Frongillo, J., Zwahlen, J., and Feng, C., "Integrated Testing of Iodine BIT-3 RF Ion Propulsion System for 6U CubeSat Applications," . Presented at the 35^{th} International Electric Propulsion Conference, Atlanta, Georgia, USA, 8-12 October 2017, IEPC-2017-264.

[19] Andreussi, T., Ferrato, E., Piragino, A., Cifali, G., Rossodivita, A., and Andrenucci, M., "DEVELOPMENT AND EXPERIMENTAL VALIDATION OF A HALL EFFECT THRUSTER RAM-EP CONCEPT," . Presented at the Space Propulsion Conference 2018, Seville, Spain, 14–18 May 2018, SP2018-00431.

[20] Barral, S., Cifali, G., Albertoni, R., Andrenucci, M., and Walpot, L., "Conceptual design of an air-breathing electric propulsion system," . Presented at The 34^{rd} International Electric Propulsion Conference, Kobe, Japan, 6–10 July 2015, IEPC-2015-271.

[21] Kimoto, Y., Yukumatsu, K., Goto, A., Miyazaki, E., and Tsuchiya, Y., "MDM: A flight mission to observe materials degradation in-situ on satellite in super low Earth orbit," *Acta Astronautica*, Vol. 179, 2021, pp. 695–701. https://doi.org/https://doi.org/10.1016/j.actaastro.2020.11.048, URL https://www.sciencedirect.com/science/article/pii/S0094576520307232.

[22] Goto, A., Umeda, K., Yukumatsu, K., and Kimoto, Y., "Property changes in materials due to atomic oxygen in the low Earth orbit," *CEAS Space Journal*, Vol. 13, No. 3, 2021, pp. 415–432. https://doi.org/10.1007/s12567-021-00376-2, URL https://doi.org/10.1007/s12567-021-00376-2.

[23] Allasio, A., Anselmi, A., Catastini, G., Cesare, S., Dumontel, M., Saponara, M., Sechi, G., Tramutola, A., Vinai, B., André, G., Fehringer, M., and Muzi, D., "GOCE MISSION: DESIGN PHASES AND IN-FLIGHT EXPERIENCES," 2010. 215th Meetin of the American Astronomical Society, Washington, DC, 3-7 January 2010, AAS-2010-081.

[24] Wallace, N., Jameson, P., Saunders, C., Fehringer, M., Edwards, C., and Floberghagen, R., "The GOCE Ion Propulsion Assembly – Lessons Learnt from the First 22 Months of Flight Operations," . Presented at the 32^{st} International Electric Propulsion Conference (IEPC), Wiesbaden, Germany, Sep. 11–15, 2011. IEPC-2011-327.

[25] Cifali, G., Misuri, T., Rossetti, P., Andrenucci, M., Valentian, D., and Feili, D., "Preliminary characterization test of HET and RIT with Nitrogen and Oxygen," 2011. 47th AIAA Joint Propulsion Conference, San Diego CA.

[26] Dukhopelnikov, D. V., Riazanov, V. A., Shilov, S. O., Manegin, D. S., and Sokolov, R. A., "Investigation of the laboratory model of a thruster with anode layer operating with air and nitrogen-oxygen mixture," *AIP Conference Proceedings*, Vol. 2318, No. 1, 2021, p. 040006. https://doi.org/10.1063/5.0036251, URL https://aip.scitation.org/doi/abs/10.1063/5.0036251.

[27] Li, Y., Chen, X., Li, D., Xiao, Y., Dai, P., and Gong, C., "Design and analysis of vacuum air-intake device used in air-breathing electric propulsion," *Vacuum*, , No. 120, 2015, pp. 89–95. https://doi.org/10.1016/j.vacuum.2015.06.011.

[28] Jackson, S. W., "Design of an Air-Breathing Electric Thruster for CubeSat Applications," Master's thesis, University of Colorado at Boulder, 2017.